Int J Clin Exp Pathol 2017;10(7):7603-7615
www.ijcep.com /ISSN:1936-2625/IJCEP0053758

Original Article

Androgen receptor antagonist bicalutamide induces autophagy and apoptosis via ULK2 upregulation in human bladder cancer cells

Kuiyuan Hao*, Sheng Zhao*, Di Cui, Yu Zhang, Chenyi Jiang, Yifeng Jing, Shujie Xia, Bangmin Han

*Department of Urology, Shanghai General Hospital, Shanghai Jiao Tong University School of Medicine, Shanghai, China. *Equal contributors.*

Received March 25, 2017; Accepted April 23, 2017; Epub July 1, 2017; Published July 15, 2017

Abstract: Studies have demonstrated a close link between autophagy and bladder cancer. The androgen receptor (AR) has also been found to be closely involved in bladder cancer progression. Although androgen ablation and AR antagonism have been proposed as potential methods for bladder cancer therapy, the mechanisms underlying their effects remain poorly understood. This study was designed to assess the effects of the AR antagonist bicalutamide on autophagy and apoptosis in bladder cancer cells. The results indicated that the AR has an inhibitory effect on autophagy in bladder cancer cells. Using different tests, we observed that bicalutamide promotes apoptosis in these cells and positively modulates autophagy in UM-UC-3 cells by upregulating ULK2. In addition, ULK2 knockdown inhibited autophagy and apoptosis in bladder cancer cells. Autophagy promotion by rapamycin enhanced apoptosis in bladder cancer cells, especially in AR-positive UM-UC-3 cells when AR signaling was inhibited by bicalutamide. These findings suggest that the AR antagonist bicalutamide induces autophagy and apoptosis in bladder cancer cells and may have potential in bladder cancer therapy because it upregulates autophagic flux by targeting the AR and its downstream gene ULK2.

Keywords: Bladder cancer, AR, bicalutamide, ULK2, autophagy, apoptosis

Introduction

Bladder cancer is characterized by significant morbidity and mortality and represents the second most frequent malignancy of the genitourinary system worldwide [1]. Estimates for the US indicate that bladder cancer will cause the deaths of 12,240 men and 4,630 women in 2017, and these values account for 20.2% and 25.0% of the newly diagnosed cases in men and women, respectively [2].

One notable characteristic of bladder cancer is the remarkable difference in morbidity between men and women, with the incidence of bladder cancer in men almost four times higher than that in women [1, 2]. Epidemiologists have demonstrated that unhealthy lifestyle choices, such as smoking, and long-term occupational exposure may be responsible for this difference. However, even when controlling for these variables, men still tend to be more prone to developing bladder cancer than women [3]. The androgen receptor (AR) and androgen signaling are considered to be connected with the etiology and progression of bladder cancer, although bladder cancer is not regarded as a traditional endocrine-related cancer [4-7]. Studies have demonstrated a high level of expression of AR in high-grade bladder cancer [8, 9]. We previously reported that AR silencing increases apoptosis in bladder cancer cells and represents a potential therapeutic target for bladder cancer [5]. However, the precise mechanism of AR antagonism in bladder cancer treatment has not been well characterized.

Macroautophagy, hereafter referred to as autophagy, is a constitutively evolutionarily conserved process during which the cytoplasm and organelles are sequestered in subcellular membranes and then delivered to the lysosome or vacuole, where they are degraded and recycled [10-12]. Autophagy is involved in the pathogen-

esis of numerous diseases, including infections, cancer, and aging [13]. The role of autophagy in the progression of bladder cancer is still the subject of debate. A previous study indicated that the human bladder cancer cell line T24 was more susceptible to apoptosis when exposed to autophagy inhibitors, such as 3-MA or chloroquine [14]. A more recent work also indicated that autophagy inhibition with bafilomycin A1 resulted in apoptosis-induced cell death in bladder cancer cell lines [15]. Moreover, autophagy has an anticancer effect. For instance, PI3K and the mTOR inhibitor NVP-BEZ235 could inhibit bladder cancer cell growth by activating autophagic flux [16]. Another relevant study showed that YM155, a novel small molecule that inhibits survivin, has significant cytotoxic effects on gemcitabine-resistant bladder cancer cell lines mediated by autophagy activation [17].

AR plays an important role in modulating autophagy in AR-dependent diseases, such as prostate cancer and benign prostate hyperplasia. A recent study indicated that AR promotes prostate cancer cell growth through autophagy downregulation [18]. By contrast, another team implicated that androgen ablation and AR inhibition by bicalutamide could induce autophagy in castration-resistant prostate cancer cells and reduce apoptosis [19]. However, the mechanism of the AR antagonist bicalutamide in the autophagic process of bladder cancer remains poorly understood. In the present study, we determined the regulatory effect of bicalutamide on the autophagy and apoptosis of bladder cancer cells and elucidated its potential mechanism of action.

Materials and methods

Cell culture and reagents

The human bladder cancer cell lines UM-UC-3 and 5637, which were obtained from the Institute of Cell Research (Chinese Academy of Sciences, Shanghai, China), were maintained in RPMI-1640 medium (HyClone, UT, USA) containing 10% fetal bovine serum (FBS) and 1% penicillin-streptomycin (Gibco, Foster City, CA, USA). All cells were cultured in a humid incubator with a 5% CO_2 atmosphere at 37°C. Unless otherwise stated, all cell samples were cultured and maintained in phenol red-free RPMI (HyClone) with 10% charcoal-stripped FBS (CFBS; HyClone) for 24 hours before being subjected to one of the treatment conditions. The treatments were performed by culturing cells for 48 hours in phenol red-free RPMI supplemented with CFBS and either 10 nM dihydrotestosterone (DHT, A8380; Sigma-Aldrich, Saint Louis) and/or 50 μM nonsteroidal bicalutamide (Bic, B9061; Sigma-Aldrich), or 100 μM chloroquine (CQ, S4157; Selleck, Shanghai, China), and/or 100 nM rapamycin (RAPA, S1039; Selleck).

Transmission electron microscopy (TEM)

After the 48-hour treatment, the cell samples were fixed with 2.5% glutaraldehyde in 0.1 M sodium cacodylate for a minimum of 2 hours and then post-fixed in osmium tetroxide for 3 hours. After gradient dehydration with ethanol, the cell samples were embedded in epon and polymerized for 48 hours at 70°C. Ultrathin sections (70 nm) were stained with uranyl acetate and lead citrate. Finally, all sections were examined using a JEM-1230 transmission electron microscope (JEOL, Tokyo, Japan) operated at 80 kV to quantify the number of autophagosomes and autophagolysosomes.

mRFP-GFP-LC3 adenovirus infection

UM-UC-3 cells were transfected with mRFP-GFP-LC3 adenovirus (Genomeditech, Shanghai, China) for 24 hours before the various treatments. All relevant operations were performed following the manufacturer's guidelines. Next, UM-UC-3 cells were exposed to the different reagents treatments for 48 hours. Finally, the nuclei were stained with DAPI. The cells were imaged using a confocal fluoresence microscope (Leica, TCS-SP8, Germany) at 400× magnification. The GFP and mRFP spots, as well as the DAPI-stained nuclei, were counted manually. The number of spots per cell was obtained by dividing the total number of spots by the number of nuclei in each microscopic field.

Stable cell line with AR and siRNA transfection

The stably overexpressing pcDNA3.1-AR cell line (5637-AR) and pcDNA3.1 vector cell line (5637-vec) were established using a previously described method [7]. The siRNAs targeting AR

Table 1. Primers and siRNAs used in the study

Application	Gene	Direction	5'-3'
qRT-PCR primers	NPC1	Forward	AAGATGGAACAAGCGTCCAG
		Reverse	TGCCCCTTGGAAGAAGTGTA
	ATG16L2	Forward	CAGTGAAGGAGTGGGACCTC
		Reverse	CCGGATCTTCTGGTCATTGT
	CTSD	Forward	GTGCTTCACAGTCGTCTTCG
		Reverse	GTGCTGGACTTGTCGCTGT
	HSPA8	Forward	CGGGCTTGTGATTGGGTCTT
		Reverse	GCCACCCTGCCTCTTATACC
	HSP90AA1	Forward	GCTCCAAGGGTTGACATGGT
		Reverse	TGTAACTCATGGACGCAGGG
	TGM2	Forward	CCAACTACAACTCGGCCCAT
		Reverse	CTGGTCATCCACGACTCCAC
	TP53	Forward	TGCTCAAGACTGGCGCTAAA
		Reverse	CAATCCAGGGAAGCGTGTCA
	ULK2	Forward	TTCCTGCTCTAAGGGTTTGCTT
		Reverse	CCAGCGAGGGAGAACAACTG
	BCL2	Forward	TTTGTGGAACTGTACGGCCC
		Reverse	GTTGACTTCACTTGTGGCCC
	RGS19	Forward	CGTCTGACTTGAGTCCCTGC
		Reverse	TGGTACCAGCTCTCAGACCC
siRNAs	siULK2-1	Sense	GCAGCACAGACAGUUUAAATT
		Antisense	UUUAAACUGUCUGUGCUGCTT
	siULK2-2	Sense	CUGACAAACAGAGGUUUAUTT
		Antisense	AUAAACCUCUGUUUGUCAGTT
	siULK2-3	Sense	CCAAUAGUCCUCAAGACUUTT
		Antisense	AAGUCUUGAGGACUAUUGGTT
	siCon	Sense	UUCUCCGAACGUGUCACGUTT
		Antisense	ACGUGACACGUUCGGAGAATT

and its control siRNA used in this study were previously described [5]. Three siRNA sequences targeting Uncoordinated 51-like kinase 2 (ULK2) and their negative control siRNA were transfected into cells using Lipofectamine 2000 (Invitrogen, Carlsbad, CA) according to the manufacturer's guidelines. The siRNA sequences are shown in **Table 1**.

Flow cytometry

Apoptosis analysis was performed using the FITC Annexin V Apoptosis Detection Kit (BD Biosciences, USA) according to the manufacturer's instructions. After different treatments, the cells were stained with Annexin V-FITC and propidium iodide (PI). The apoptotic level of the cells was assessed by a BD Accuri C6 flow cytometer (BD Biosciences).

Hoechst staining

Cell apoptosis was detected using Hoechst staining (Beyotime Biotechnology, Shanghai, China). The UM-UC-3 cells were seeded in 6-well plates and then subjected to different treatments. Next, the UM-UC-3 cells were stained with Hoechst for 30 min and washed with phosphate-buffered saline (PBS) for 5 min 3 times. Finally, the cell samples were observed and imaged using a fluorescence microscope (Leica, DMi8, Germany).

RNA extraction and quantitative real-time polymerase chain reaction (qRT-PCR)

The total RNA of the cells was prepared using TRIzol reagent (Life Technologies, Foster City, CA, USA) according to the manufacturer's protocols. Reverse transcription of the mRNA was performed using the PrimeScript RT Master Mix (Takara, Otsu, Shiga, Japan). Quantitative real-time PCR was conducted using the SYBR Premix Ex Taq (Takara). GAPDH was used as an internal control. Detailed information about the primer pairs is shown in **Table 1**. The relative mRNA expression was calculated based on the $2^{-\Delta\Delta Ct}$ method.

Protein extraction and western blotting

After a series of treatments, the total protein content was extracted from the UM-UC-3 or 5637 cells. Western blotting was performed as previously described [7] with slight modifications. The proteins (20-40 μg) were separated on 10% or 12% SDS-PAGE gels and then transferred onto PVDF membranes (Roche). The primary antibodies for β-actin (4970, rabbit), AR (5153, rabbit), Bcl-2 (2872, rabbit), cleaved caspase-3 (9664, rabbit), and LC3-I/II (4108, rabbit) were obtained from Cell Signaling Technology, Inc. The primary antibody for ULK2 (ab211632, rabbit) was purchased from Abcam, Inc.

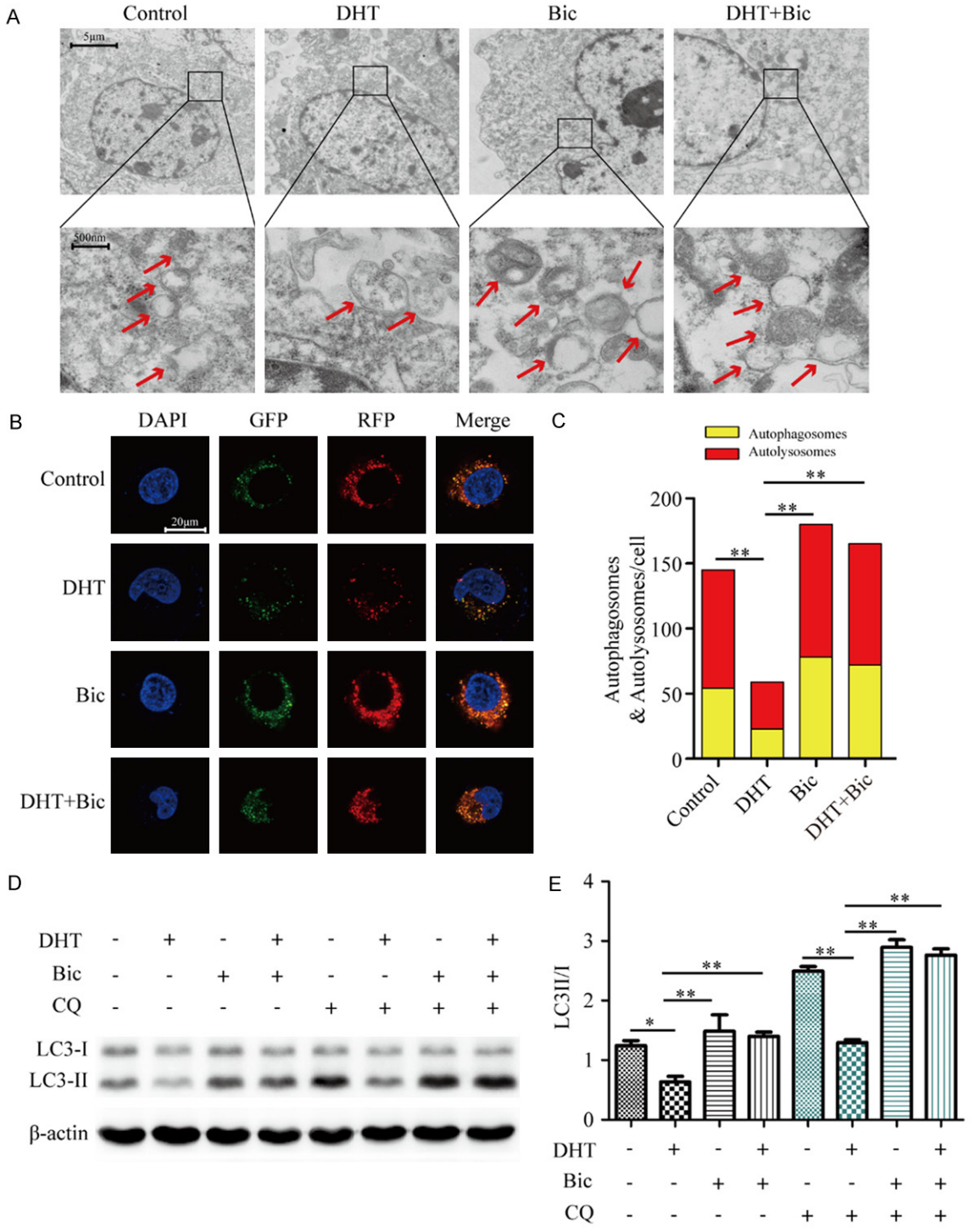

Figure 1. Effects of DHT and Bic treatment on the autophagic flux in UM-UC-3 cells. A. Transmission electron microscopy was used to detect autophagosomes and autolysosomes in UM-UC-3 cells that were cultured in 10 nM DHT and (or) 50 μM Bic for 48 h. B. Fluorescence microscopy analysis of UM-UC-3 cells transiently infected with mRFP-GFP-LC3 adenovirus and then cultured with 10 nM DHT and/or 50 μM Bic for 48 h. Scale bar = 20 μm. C. Quantification of RFP-LC3 spots and merged spots demonstrating autophagy flux was inhibited by 10 nM DHT. D and E. Immunoblot analysis and densitometry assessing the LC3 conversion ratio (LC3-II/I) in UM-UC-3 cells treated with 10 nM DHT and/or 50 μM Bic for 48 h and before and after the inhibition of LC3-II degradation by 100 μM chloroquine. β-actin immunodetection was used as an internal control (*P<0.05, **P<0.01).

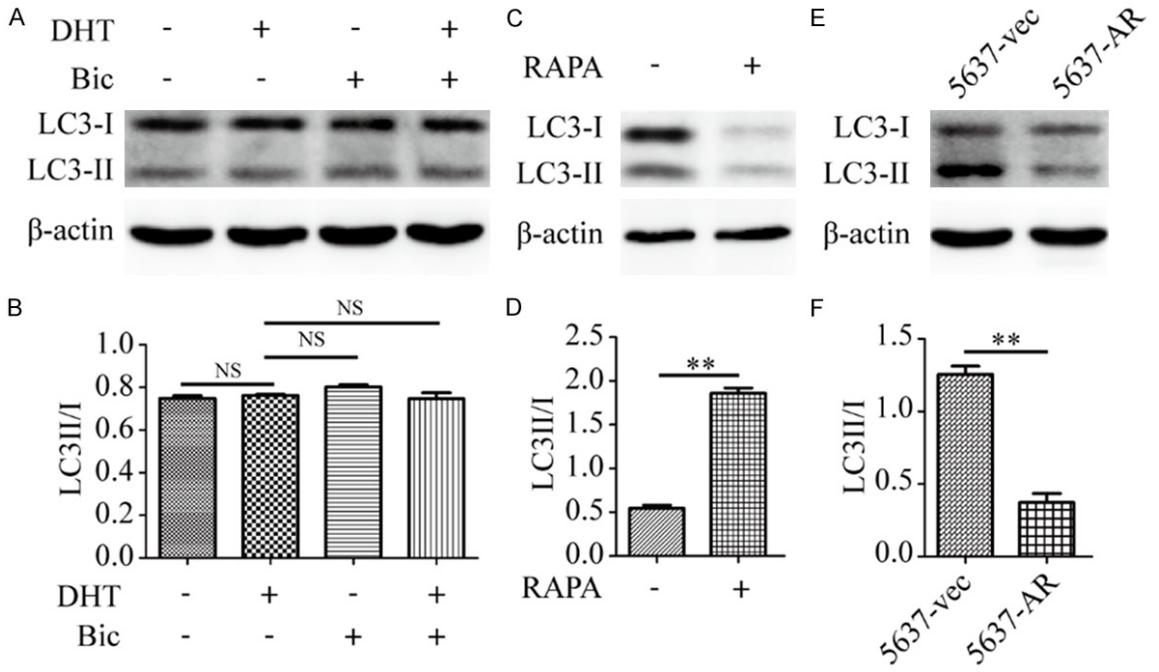

Figure 2. Assessment of the effect of DHT and Bic on the autophagic flux of AR-deficient 5637 cells. A and B. Immunoblot analysis and densitometry assessment of the LC3 conversion ratio (LC3-II/I) in 5637 cells treated with 10 nM DHT and/or 50 μM Bic for 48 h. C and D. Immunoblot analysis and densitometry assessment of the LC3 conversion ratio (LC3-II/I) in 5637 cells treated with 100 nM rapamycin. E and F. Immunoblot analysis and densitometry assessment of the LC3 conversion ratio (LC3-II/I) in 5637 cells stably overexpressing AR (5637-AR) or vector (5637-vec) under a treatment of 10 nM DHT (NS = not significant, $**P<0.01$).

Statistical analysis

All experiments were conducted at least three times. Statistical analyses were performed using the Statistical Package for the Social Sciences software version 19.0 (SPSS, Inc., Chicago, IL, USA). Statistical significance was set at $P<0.05$. The data were analyzed by performing a one-way ANOVA or a two-sided Student's t-test.

Results

Androgen blockade induces autophagy in AR-positive bladder cancer cells

To assess the effect of AR antagonism on bladder cancer cell autophagy, we first cultured and maintained AR-positive UM-UC-3 cells and AR-negative 5637 cells for our experiments [7, 20]. To monitor cellular autophagy, three classical approaches were used, including TEM, confocal laser scanning microscopy, and western blot assays [21]. We treated UM-UC-3 cells for 48 hours with DHT and Bic alone or in combination. The double or multiple membranes of autophagic vesicles (autophagosomes and autolysosomes), which are considered hallmarks of autophagy, were detected by TEM. We found more autophagic vesicles in vehicle-treated UM-UC-3 cells and those treated with Bic than in DHT-treated cells (**Figure 1A**). Furthermore, the number of autophagosomes (yellow spots) and autolysosomes (red spots, merged red spots and green spots) increased after exposure to Bic (**Figure 1B**, **1C**). Western blots showed that the Bic treatment group had a greater LC3 conversion ratio than the DHT groups, as indicated by the LC3-II/LC3-I ratio before and after the inhibition of LC3-II degradation by chloroquine (**Figure 1D**, **1E**).

To rule out the possibility that the increased level of autophagy from Bic treatment could be an off-target effect, the same treatments were applied to AR-negative 5637 cells. As expected, the treatments with DHT or Bic did not affect the LC3 conversion in 5637 cells, which suggested that the autophagy induced by Bic in UM-UC-3 cells was mediated by the AR (**Figure 2A**, **2B**). The functionality of the autophagic

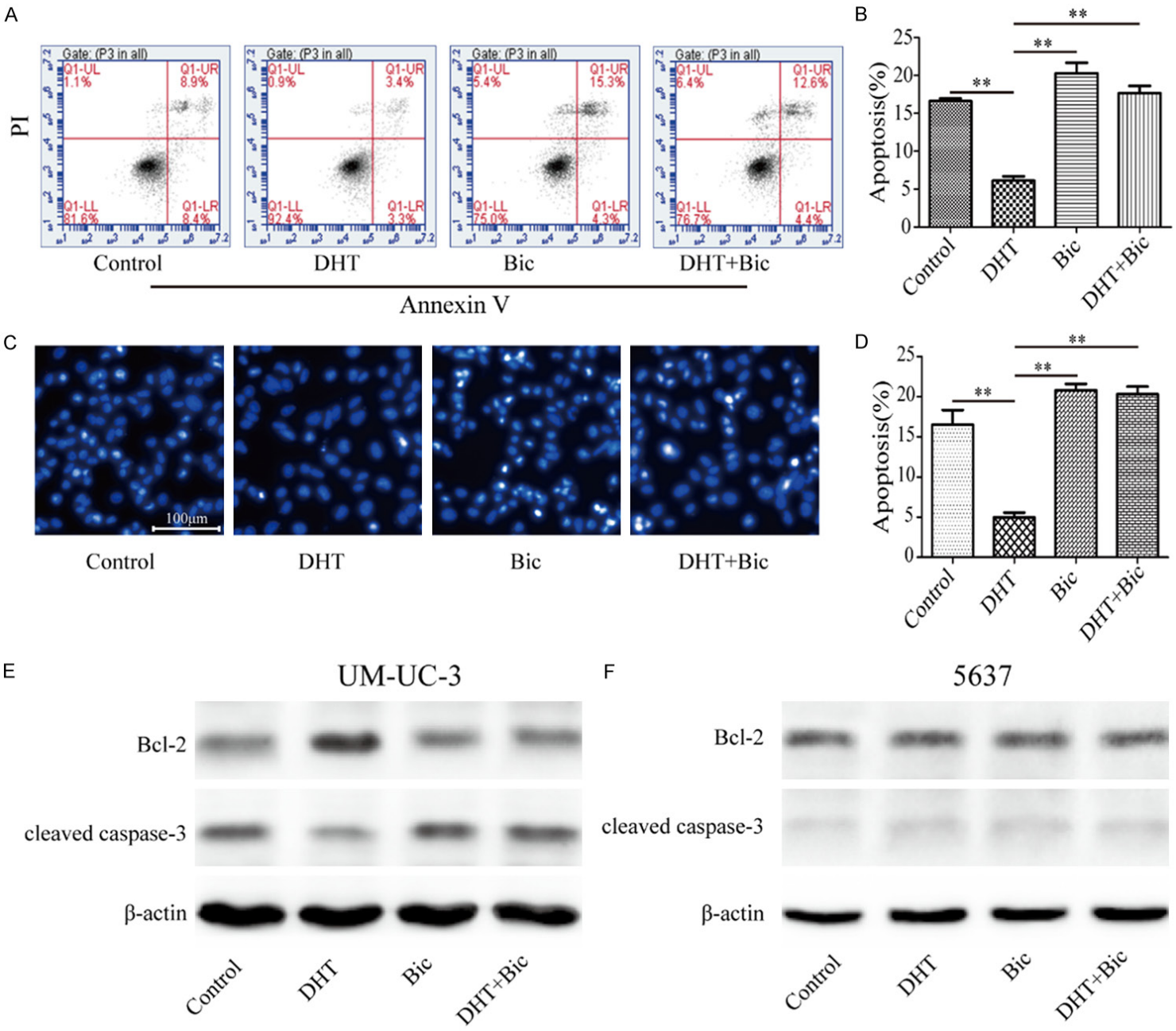
A
PI
Annexin V
Gate: (P3 in all)
Q1-UL 1.1%
Q1-UR 8.9%
Q1-LL 81.6%
Q1-LR 8.4%
Q1-UL 0.9%
Q1-UR 3.4%
Q1-LL 92.4%
Q1-LR 3.3%
Q1-UL 5.4%
Q1-UR 15.3%
Q1-LL 75.0%
Q1-LR 4.3%
Q1-UL 6.4%
Q1-UR 12.6%
Q1-LL 76.7%
Q1-LR 4.4%
Control
DHT
Bic
DHT+Bic
B
Apoptosis(%)
25
20
15
10
5
0
**
**
**
Control
DHT
Bic
DHT+Bic
C
100μm
Control
DHT
Bic
DHT+Bic
D
Apoptosis(%)
25
20
15
10
5
0
**
**
**
Control
DHT
Bic
DHT+Bic
E
UM-UC-3
Bcl-2
cleaved caspase-3
β-actin
Control
DHT
Bic
DHT+Bic
F
5637
Bcl-2
cleaved caspase-3
β-actin
Control
DHT
Bic
DHT+Bic

Figure 3. Apoptosis analysis of UM-UC-3 or 5637 cells after DHT and Bic treatment. A and B. Flow cytometry detected apoptosis inhibition by 10 nM DHT compared with the control or 50 μM Bic treatment. C. Hoechst staining revealed apoptosis inhibition by 10 nM DHT compared with the control or 50 μM Bic treatment. Scale bar = 100 μm. D. Quantitative analysis of Hoechst staining results to assess the percentage of apoptotic cells. E and F. Immunoblot analysis of Bcl-2 and cleaved caspase-3 in UM-UC-3 or 5637 cells treated with 10 nM DHT and/or 50 μM Bic for 48 h (**P<0.01).

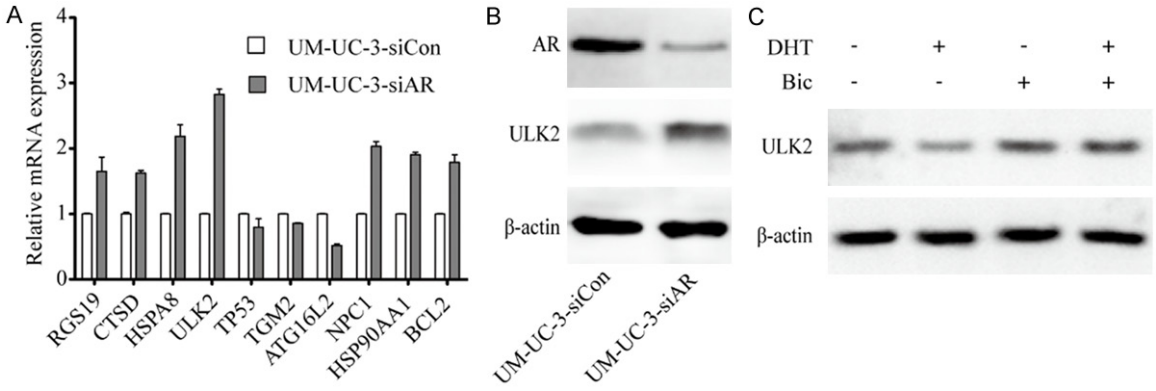

Figure 4. ULK2 expression in UM-UC-3 cells. A. qRT-PCR results showing changes in the mRNA expression of ten ATGs in UM-UC-3 cells after AR knockdown. B. Immunoblot analysis detected increased ULK2 expression in UM-UC-3 cells after AR knockdown. C. Immunoblot analysis assessing the ULK2 expression in UM-UC-3 cells after treatment with 10 nM DHT and/or 50 μM Bic for 48 h.

pathways in 5637 cells was supported by the increased LC3 conversion with treatment with the positive control, RAPA (**Figure 2C**, **2D**). Furthermore, 5637-AR cells showed less LC3 conversion than 5637-vec cells after treatment with DHT (**Figure 2E**, **2F**). These findings indicated that the inactivation of AR signaling by Bic promotes autophagy in AR-positive bladder cancer cells.

Androgen blockade induces apoptosis in UM-UC-3 cells

To test the effect of inactivated androgen signaling on bladder cancer cell apoptosis, we first analyzed the percentage of apoptotic cells using flow cytometry. After treatment with Bic for 48 hours, the apoptotic cells increased notably compared with those in the DHT group (**Figure 3A**, **3B**). The apoptotic levels were also confirmed by Hoechst staining. As shown, the Bic and control groups appeared to have higher levels of apoptosis than did the DHT group (**Figure 3C**, **3D**). We also detected the increased cleavage of caspase-3 and decreased Bcl-2 expression after androgen blockade using western blotting (**Figure 3E**). In addition, the treatments with DHT or Bic did not affect the expression of Bcl-2 and the cleavage of caspase-3 in 5637 cells (**Figure 3F**). Collectively, the results above demonstrated that the AR competitor Bic induces apoptosis in UM-UC-3 cells.

Expression of ULK2 increases after AR knockdown in UM-UC-3 cells

Previous studies have shown that AR signaling participates in different steps of autophagy in prostate cancer cells [18, 19], although few have focused on the crosstalk between AR signaling and autophagy-related genes (ATGs). Here, we performed RNA transcriptome sequencing from control cells or cells treated with siRNAs against AR. Ten ATGs with obvious changes were then quantified using qRT-PCR (**Figure 4A**). We focused on ULK2, which increased significantly by AR knockdown. The qPCR results were further verified by western blotting (**Figure 4B**). Furthermore, the results after treatment with the AR agonist DHT or antagonist Bic were consistent with the results indicated above (**Figure 4C**).

ULK2 promotes autophagy in UM-UC-3 cells

Several studies have shown that ULK2 plays an important role in autophagosome formation

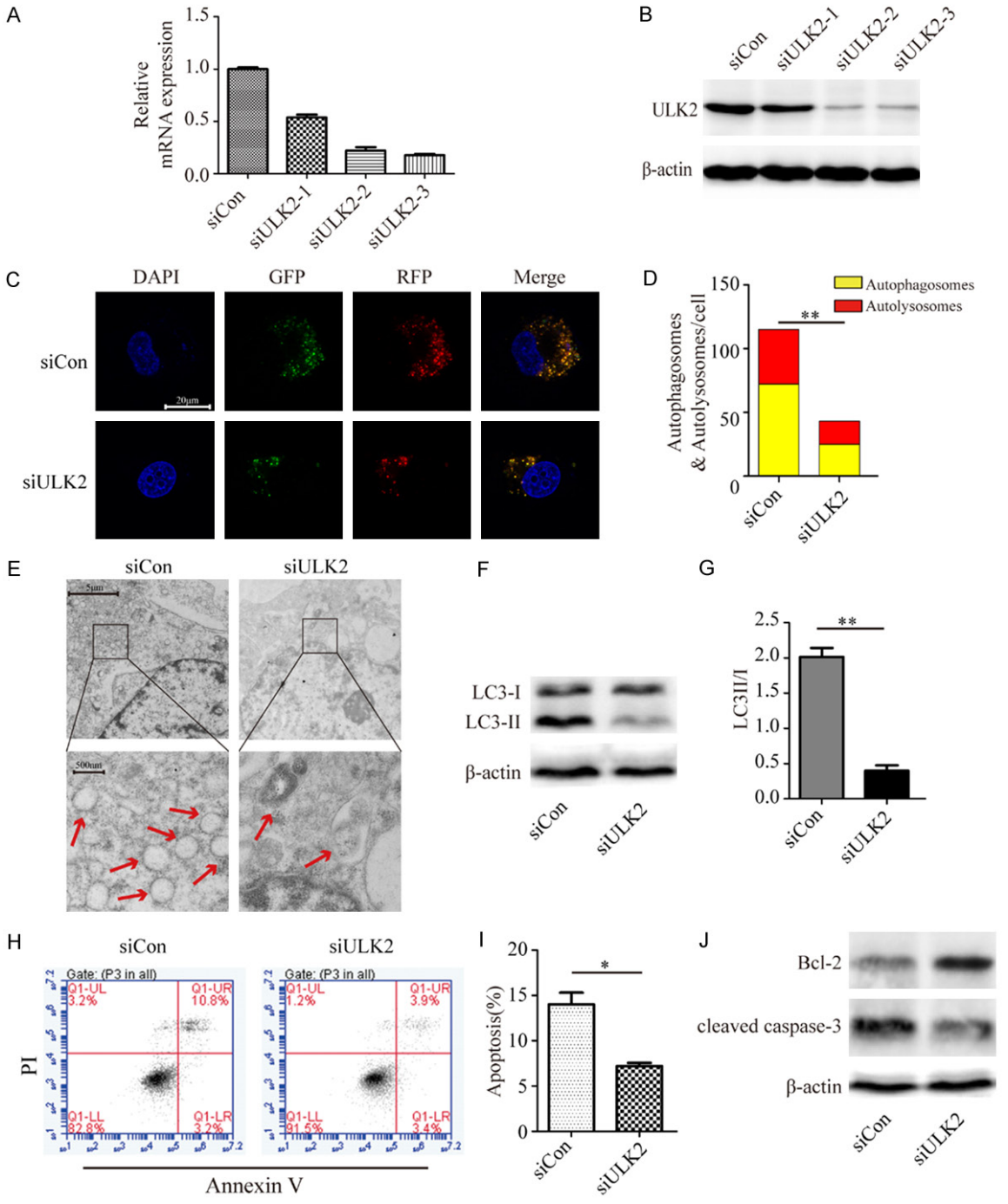

Figure 5. Effect of ULK2 on the autophagic flux and apoptosis of UM-UC-3 cells. A and B. qRT-PCR and immunoblot analysis results showing changes in the ULK2 expression with three different siRNA sequences. The results revealed that siULK2-3 had the highest knockdown efficiency. C. Fluorescence microscopy analysis of UM-UC-3 cells transiently infected with mRFP-GFP-LC3 adenovirus and then transfected with an siRNA targeting ULK2 or a negative control siRNA. Scale bar = 20 μm. D. Quantification of the RFP-LC3 spots and merged spots demonstrating decreased autophagic flux in UM-UC-3 cells after ULK2 knockdown. E. Transmission electron microscopy results for the detection of autophagosomes and autolysosomes in UM-UC-3 cells that were transfected with an siRNA targeting ULK2 or a negative control siRNA. F and G. Immunoblot analysis and densitometry assessing the LC3 conversion ratio (LC3-II/I) of UM-UC-3 cells that were transfected with siRNA targeting ULK2 or negative control siRNA. H and I. Flow cytometry was used to detect decreased apoptosis in UM-UC-3 cells after ULK2 knockdown. J. Immunoblot analysis of Bcl-2 and cleaved caspase-3 in UM-UC-3 cells transfected with siRNA targeting ULK2 or negative control siRNA (*P<0.05, **P<0.01).

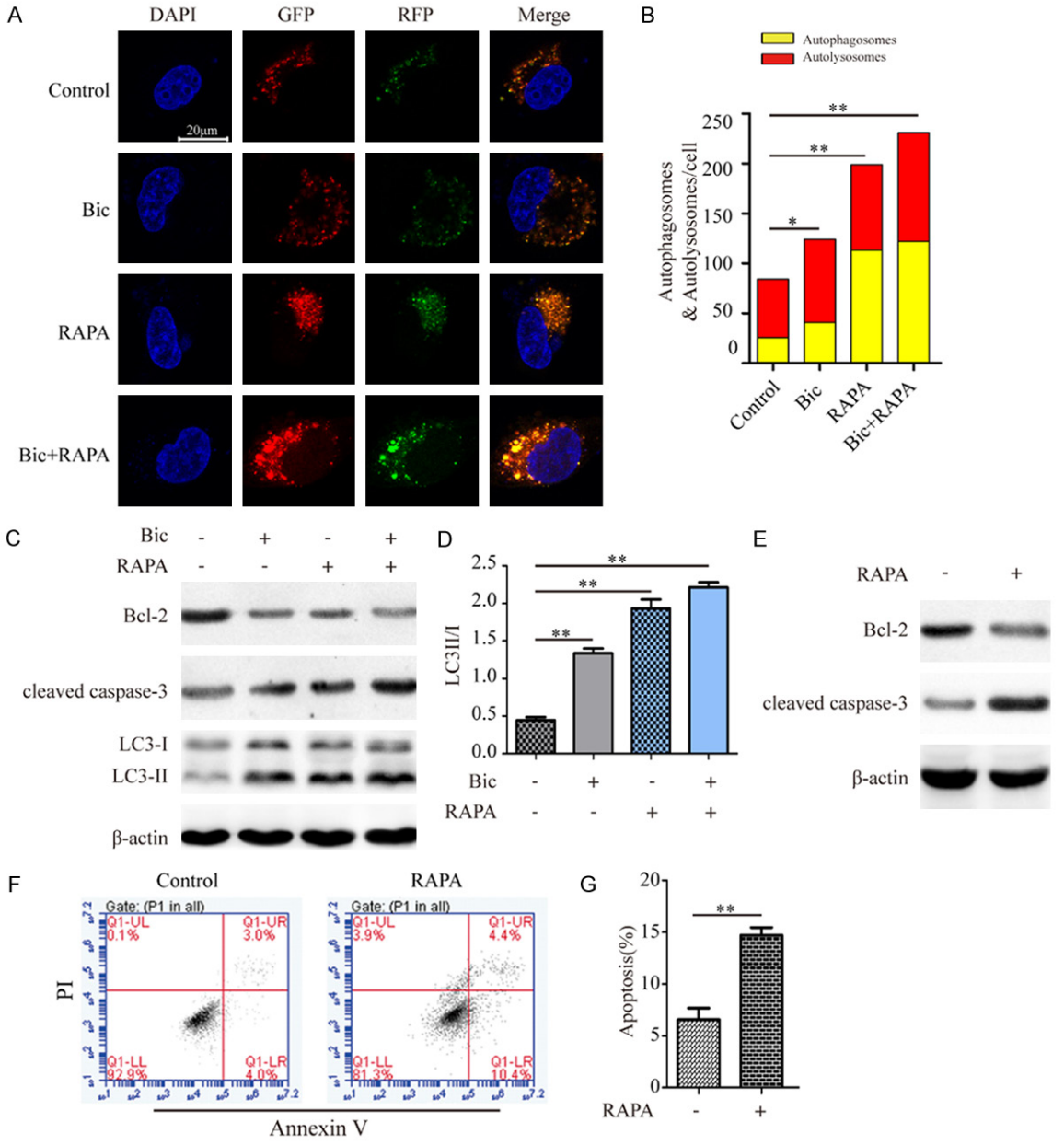

Figure 6. Effect of the excessive autophagy induced by RAPA with or without Bic on the apoptosis of UM-UC-3 and 5637 cells. A. Fluorescence microscopy analysis of UM-UC-3 cells transiently infected with mRFP-GFP-LC3 adenovirus and then treated with 100 nM rapamycin and/or 50 μM bicalutamide for 48 h. Scale bar = 20 μm. B. Quantification of the RFP-LC3 spots and merged spots demonstrating the substantial autophagic flux in UM-UC-3 cells treated with 100 nM rapamycin accompanied by 50 μM bicalutamide. C. Immunoblot analysis of apoptosis-related proteins and the LC3 conversion of UM-UC-3 cells in different conditions. D. Densitometry assessing the LC3 conversion ratio (LC3-II/I) of UM-UC-3 cells under different conditions. E. Immunoblot analysis of the apoptosis-related proteins in 5637 cells after treatment with 100 nM rapamycin. F and G. Flow cytometry analysis detected increased apoptosis in 5637 cells after treatment with 100 nM rapamycin (*P<0.05, **P<0.01).

[22-24]. To assess the effect of ULK2 on the autophagy of UM-UC-3 cells, we transiently silenced ULK2 via the transfection of specific siRNAs into UM-UC-3 cells. Among three distinct designed siRNAs, siULK2-3 possessed the highest knockdown efficiency (**Figure 5A**, **5B**). SiULK2-3 was used for subsequent experiments. The results suggested that ULK2 silencing suppressed UM-UC-3 cell autophagy, as demonstrated by significantly decreased

amounts of fluorescent spots (**Figure 5C**, **5D**). In addition, TEM detected fewer autophagosomes and autolysosomes in ULK2 knocked-down UM-UC-3 cells than in control cells (**Figure 5E**). The decreased ratio of LC3 II/LC3 I also verified these results (**Figure 5F**, **5G**). Thus, the three independent assays (the formation of mRFP-GFP-LC3 spots, LC3 turnover, and TEM assays) all suggested that the decreased expression of ULK2 resulting from the activated AR may explain the inhibition of autophagy in UM-UC-3 cells.

ULK2 promotes apoptosis in UM-UC-3 cells

To explore the effect of ULK2 on apoptosis in UM-UC-3 cells, we employed flow cytometry and western blotting to detect the apoptotic levels of cells with or without ULK2 silencing. The flow cytometry analysis showed a decreased number of apoptotic cells in the population of the ULK2-knocked-down UM-UC-3 cells (**Figure 5H**, **5I**). Moreover, the apoptotic protein analysis showed that the knockdown of ULK2 significantly inhibited apoptosis in UM-UC-3 cells (**Figure 5J**).

Promotion of autophagy enhances bladder cancer cell apoptosis

Early studies demonstrated that autophagy plays an important role in bladder cancer progression [15-17]. Thus, we tested whether increased autophagy could enhance bladder cancer cell apoptosis. UM-UC-3 and 5637 cells were cultured in RPMI-1640 medium containing 10% FBS and 1% penicillin-streptomycin. The results showed that AR competition by Bic accompanied by RAPA exhibited stronger autophagy activity in UM-UM-3 cells than any other treatment, as shown by the significantly increased fluorescent spots and the LC3 conversion ratio (LC3-II/LC3-I) (**Figure 6A-D**). In addition, the western blot results revealed intensive autophagy augmented apoptosis in UM-UC-3 cells (**Figure 6C**). The promotion of autophagy by RAPA also significantly increased 5637 cell apoptosis (**Figures 2C**, **2D**, **6E-G**). Thus, these results suggested that autophagy promotion enhanced apoptosis in bladder cells.

Discussion

In the present study, we confirmed that the AR antagonist bicalutamide promotes autophagy and apoptosis in bladder cancer cells by upregulating the expression of ULK2. A combination of the AR competitor Bic and the mTOR inhibitor RAPA significantly enhanced apoptosis in bladder cancer cells via autophagy induction.

Increasing evidence indicates that the different levels of androgens and AR between men and women may account for the gender disparity in bladder cancer. An earlier study indicated that AR knockout mice could not develop BBN-induced bladder cancer, whereas 25% AR knockout mice developed BBN-induced tumors with the exogenous supplementation of DHT [20]. Another study found that bladder tumor progression was significantly inhibited by selectively ablating AR in urothelial tissue [25]. Furthermore, AR expression was notably higher in bladder tumors than in normal bladder tissue, and patients with AR-negative tumors had a better prognosis than those with AR-positive tumors [26]. In this study, our results showed that AR inactivation by Bic increased apoptosis in bladder cancer cells, which is consistent with the results of our previous study [5]. Thus, the underlying mechanisms must be determined because of the vital role of AR in the development of bladder cancer.

In general, autophagy acts as a “double-edged sword” in the fate of many cancers, including bladder cancer. The basal level of autophagy maintains the homeostasis of eukaryotes by selectively degrading redundant, aged, and damaged organelles and proteins, whereas inappropriate levels of autophagy promote apoptosis or necrosis in cancer cells, which leads to autophagic cell death [12]. An earlier study suggested that several mTOR signaling-related tumor suppressor genes, such as PTEN, TSC2, and p53, also stimulate autophagy [27]. Furthermore, another study found that the depletion of the autophagy-specific gene Beclin 1 resulted in increased tumorigenesis in mice [28]. In addition, ATG5 and Beclin 1 were found to upregulate and promote autophagic cell death following the overexpression of oncogenic RAS [29, 30]. Several studies have demonstrated the anticancer effect of autophagy [16, 17]. Moreover, the overexpression of miRNA-222 significantly inhibited autophagy and cisplatin-mediated cytotoxicity in the 5637 and T24 bladder cancer cell lines [31]. Our study detected a lower autophagy signal in the DHT group

than in any other group of AR-positive UM-UC-3 cells, whereas significant differences in autophagy activities were not detected in AR-negative 5637 cells with DHT or Bic treatment. These results indicate the positive role of AR antagonism in the regulation of autophagy in bladder cancer cells, and they are further supported by the results observed after overexpressing AR in 5637 cells and monitoring the autophagy flux after treatment with DHT. As expected, the overexpression of AR inhibited autophagy in 5637 cells.

Considerable evidence indicates that the process of autophagy is regulated by various ATGs. We found that impairing AR influences autophagy in bladder cells by regulating ATG expression. In this study, we found that the mRNA and protein levels of ULK2 were upregulated after AR knockdown in UM-UC-3 cells. Furthermore, the expression of ULK2 decreased with DHT treatment when compared with the control. ULK2 is a mammalian homolog of *Saccharomyces cerevisiae* Atg1 and is considered an upstream initiator of autophagy [24]. Dephosphorylated ULK2 first interacts with Atg13 and FIP200 and then activates autophagy by recruiting other ATG proteins, such as LC3 and Atg16, to the autophagosome formation site [32, 33]. ULK2 is involved in apoptosis through the p53 pathway [34]. Sudhanshu Shukla et al. reported that methylation-mediated silencing of ULK2 is important for glioblastoma progression, which indicates the essential role of ULK2 in autophagy and apoptosis [35]. However, the pathophysiologic role of ULK2 in bladder cancer remains unclear. In our experiments, we found that ULK2 promoted autophagy and apoptosis in UM-UC-3 cells. By silencing ULK2 with a specific siRNA, we detected a decrease in the autophagic flux and in the apoptosis of UM-UC-3 cells, which indicated that the positive effect of inactivated AR signaling by Bic on the autophagy and apoptosis of bladder cancer cells was partially caused by the upregulation of ULK2. In addition, our results demonstrated that Bic and/or RAPA enhanced bladder cancer cell apoptosis by inducing autophagy.

In conclusion, our study provides a potential mechanism that explains how inactivated AR signaling inhibits bladder cancer progression via autophagy and apoptosis induction. The combined targeting of the AR with bicalutamide and the application of RAPA may be a potential approach for inhibiting bladder cancer progression.

Acknowledgements

This work was supported by the National Natural Science Foundation of China (81372754 and 81300625).

Disclosure of conflict of interest

None.

Address correspondence to: Dr. Bangmin Han, Department of Urology, Shanghai General Hospital, Hongkou District, 100 Haining Road, Shanghai, China. Tel: +86 21 63240090; Fax: 21 63240825; E-mail: hanbm@163.com

References

[1] Torre LA, Bray F, Siegel RL, Ferlay J, Lortet-Tieulent J and Jemal A. Global cancer statistics, 2012. Ca Cancer J Clin 2015; 65: 87-108.

[2] Siegel RL, Miller KD and Jemal A. Cancer statistics, 2017. Ca Cancer J Clin 2017; 66: 7-30.

[3] Hartge P, Harvey EB, Linehan WM, Silverman DT, Sullivan JW, Hoover RN and Fraumeni JF Jr. Unexplained excess risk of bladder cancer in men. J Natl Cancer Inst 1990; 82: 1636-1640.

[4] Li Y, Izumi K and Miyamoto H. The role of the androgen receptor in the development and progression of bladder cancer. Jpn J Clin Oncol 2012; 42: 569-577.

[5] Wu JT, Han BM, Yu SQ, Wang HP and Xia SJ. Androgen receptor is a potential therapeutic target for bladder cancer. Urology 2010; 75: 820-827.

[6] Shiota M, Takeuchi A, Yokomizo A, Kashiwagi E, Tatsugami K, Kuroiwa K and Naito S. Androgen receptor signaling regulates cell growth and vulnerability to doxorubicin in bladder cancer. J Urol 2012; 188: 276-286.

[7] Jing Y, Cui D, Guo W, Jiang J, Jiang B, Lu Y, Zhao W, Wang X, Jiang Q and Han B. Activated androgen receptor promotes bladder cancer metastasis via Slug mediated epithelial-mesenchymal transition. Cancer Lett 2014; 348: 135-145.

[8] Zhuang YH, Bläuer M, Tammela T and Tuohimaa P. Immunodetection of androgen receptor in human urinary bladder cancer. Histopathology 1997; 30: 556-562.

[9] Birtle AJ, Freeman A and Munson P. The androgen receptor revisited in urothelial carcinoma. Histopathology 2004; 45: 98-99.

[10] Yorimitsu T and Klionsky DJ. Autophagy: molecular machinery for self-eating. Cell Death Differ 2005; 12 Suppl 2: 1542-1552.
[11] Beth Levine GK. Autophagy in the pathogenesis of disease. Cell 2008; 132: 27-42.
[12] Mariño G, Niso-Santano M, Baehrecke EH and Kroemer G. Self-consumption: the interplay of autophagy and apoptosis. Nat Rev Mol Cell Biol 2014; 15: 81-94.
[13] Klionsky DJ and Emr SD. Autophagy as a regulated pathway of cellular degradation. Science 2000; 290: 1717-1721.
[14] Ojha R, Singh SK, Bhattacharyya S, Dhanda RS, Rakha A, Mandal AK and Jha V. Inhibition of grade dependent autophagy in urothelial carcinoma increases cell death under nutritional limiting condition and potentiates the cytotoxicity of chemotherapeutic agent. J Urol 2014; 191: 1889-1898.
[15] Lin YC, Lin JF, Wen SI, Yang SC, Tsai TF, Chen HE, Chou KY and Hwang TI. Inhibition of high basal level of autophagy induces apoptosis in human bladder cancer cells. J Urol 2015; 195: 1126-1135.
[16] Li JR, Cheng CL, Yang CR, Ou YC, Wu MJ and Ko JL. Dual inhibitor of phosphoinositide 3-kinase/mammalian target of rapamycin NVP-BEZ235 effectively inhibits cisplatin-resistant urothelial cancer cell growth through autophagic flux. Toxicol Lett 2013; 220: 267-276.
[17] Huang YT, Cheng CC, Lin TC, Chiu TH and Lai PC. Therapeutic potential of sepantronium bromide YM155 in gemcitabine-resistant human urothelial carcinoma cells. Oncol Rep 2013; 31: 179-190.
[18] Jiang Q, Yeh S, Wang X, Xu D, Zhang Q, Wen X, Xia S and Chang C. Targeting androgen receptor leads to suppression of prostate cancer via induction of autophagy. J Urol 2012; 188: 1361-1368.
[19] Boutin B, Tajeddine N, Versmissen P, Zanou N, Schoor MV, Mondin L, Courtoy PJ, Tombal B and Gailly P. Androgen deprivation and androgen receptor competition by bicalutamide induce autophagy of hormone-resistant prostate cancer cells and confer resistance to apoptosis. Prostate 2013; 73: 1090-1102.
[20] Miyamoto H, Yang Z, Chen YT, Ishiguro H, Uemura H, Kubota Y, Nagashima Y, Chang YJ, Hu YC and Tsai MY. Promotion of bladder cancer development and progression by androgen receptor signals. J Natl Cancer Inst 2007; 99: 558-568.
[21] Wang Y, Liu J, Tao Z, Wu P, Cheng W, Du Y, Zhou N, Ge Y and Yang Z. Exogenous HGF prevents cardiomyocytes from apoptosis after hypoxia via up-regulating cell autophagy. Cell Physiol Biochem 2016; 38: 2401-2413.
[22] Jung CH, Jun CB, Ro SH, Kim YM, Otto NM, Cao J, Kundu M and Kim DH. ULK-Atg13-FIP200 complexes mediate mTOR signaling to the autophagy machinery. Mol Biol Cell 2009; 20: 1992-2003.
[23] Chan EYW and Tooze SA. Kinase-inactivated ULK proteins inhibit autophagy via their conserved C- terminal domains using an Atg13-independent mechanism. Mol Cell Biol 2009; 29: 157-171.
[24] Lee EJ and Tournier C. The requirement of uncoordinated 51-like kinase 1 (ULK1) and ULK2 in the regulation of autophagy. Autophagy 2011; 7: 689-695.
[25] Hsu JW, Hsu I, Xu D, Miyamoto H, Liang L, Wu XR, Shyr CR and Chang C. Decreased tumorigenesis and mortality from bladder cancer in mice lacking urothelial androgen receptor. Am J Pathol 2013; 182: 1811-1820.
[26] Mashhadi R, Pourmand G, Kosari F, Mehrsai A, Salem S, Pourmand MR, Alatab S, Khonsari M, Heydari F and Beladi L. Role of steroid hormone receptors in formation and progression of bladder carcinoma: a case-control study. Urol J 2014; 11: 1968-1973.
[27] Botti J, Djavaheri-Mergny M, Pilatte Y and Codogno P. Autophagy signaling and the cogwheels of cancer. Autophagy 2006; 2: 67-73.
[28] Qu X, Yu J, Bhagat G, Furuya N, Hibshoosh H, Troxel A, Rosen J, Eskelinen EL, Mizushima N and Ohsumi Y. Promotion of tumorigenesis by heterozygous disruption of the beclin 1 autophagy gene. J Clinical Invest 2003; 112: 1809-1820.
[29] Byun JY, Yoon CH, An S, Park IC, Kang CM, Kim MJ and Lee SJ. The Rac1/MKK7/JNK pathway signals upregulation of Atg5 and subsequent autophagic cell death in response to oncogenic Ras. Carcinogenesis 2009; 30: 1880-1888.
[30] Elgendy M, Sheridan C, Brumatti G and Martin SJ. Oncogenic ras-induced expression of noxa and Beclin-1 promotes autophagic cell death and limits clonogenic survival. Mol Cell 2011; 42: 23-35.
[31] Zeng LP, Hu ZM, Li K and Xia K. miR-222 attenuates cisplatin-induced cell death by targeting the PPP2R2A/Akt/mTOR Axis in bladder cancer cells. J Cell Mol Med 2016; 20: 559-567.
[32] Wong PM, Puente C, Ganley IG and Jiang X. The ULK1 complex: sensing nutrient signals for autophagy activation. Autophagy 2013; 9: 124-137.
[33] Hara T, Takamura A, Kishi C, Iemura S, Natsume T, Guan JL and Mizushima N. FIP200, a ULK-interacting protein, is required for autophagosome formation in mammalian cells. J Cell Biol 2008; 181: 497-510.

[34] Yang MH, Yoo KH, Yook YJ, Park EY, Jeon JO, Choi SH, Park SY, Woo YM, Lee MJ and Park JH. The gene expression profiling in murine cortical cells undergoing programmed cell death (PCD) induced by serum deprivation. J Biochem Mol Biol 2007; 40: 277-285.

[35] Shukla S, Patric IR, Patil V, Shwetha SD, Hegde AS, Chandramouli BA, Arivazhagan A, Santosh V and Somasundaram K. Methylation silencing of ULK2, an autophagy gene, is essential for astrocyte transformation and tumor growth. J Biol Chem 2014; 289: 22306-22318.